Supersilicic clinopyroxene and silica exsolution in UHPM eclogite and pelitic gneiss from the Kokchetav massif, Kazakhstan

5 authors, including:

Ikuo Katayama
Hiroshima University
143 PUBLICATIONS   6,382 CITATIONS

SEE PROFILE

Kazuaki Okamoto
Saitama University
57 PUBLICATIONS   1,573 CITATIONS

SEE PROFILE

Shigenori Maruyama
Tokyo Institute of Technology
537 PUBLICATIONS   21,259 CITATIONS

SEE PROFILE

Some of the authors of this publication are also working on these related projects:

Project P-T paths and extent of hydration deduced from amphibole zoning View project

Project Physical properties of uppermost mantle structure and the Mohorovicic seismic discontinuity View project

Supersilicic clinopyroxene and silica exsolution in UHPM eclogite and pelitic gneiss from the Kokchetav massif, Kazakhstan

IKUO KATAYAMA,[1,*] CHRISTOPHER D. PARKINSON,[1] KAZUAKI OKAMOTO,[1] YOUICHI NAKAJIMA,[2] AND SHIGENORI MARUYAMA[1]

[1]Department of Earth and Planetary Sciences, Tokyo Institute of Technology, Tokyo 152-8551, Japan
[2]Institute of Earth Science, Waseda University, Tokyo 169-8050, Japan

ABSTRACT

Abundant exsolved quartz rods occur in matrix clinopyroxene of eclogite from the Kokchetav massif, Kazakhstan. These rocks are diamond-grade, ultrahigh-pressure (UHP) metamorphic rocks that recrystallized at $P > 6$ GPa and $T > 1000$ °C. Zircon is an excellent container, which effectively protects peak UHP metamorphic phases from retrogression. Therefore, to ascertain the pre-exsolution composition of the clinopyroxene, we analyzed clinopyroxene inclusions in zircon of the eclogite and a diamond-bearing biotite gneiss. Clinopyroxene in zircon has an excess of $Fe^{3+} + {}^{VI}Al$ over ${}^{IV}Al$ + Na + K, and calculated cation totals significantly less than 4.0 per six O atoms. The stoichiometry of these pyroxenes can be reconciled if the Ca-Eskola end-member ($Ca_{0.5}\square_{0.5}AlSi_2O_6$) is considered. The zircon-hosted clinopyroxene in the eclogite contains up to 9.6 mol% of the Ca-Eskola component, and in the biotite gneiss up to 18.2 mol%, whereas the matrix clinopyroxene contains much less (1.3 mol%, on average). Recalculation of the composition of the matrix clinopyroxene prior to exsolution of quartz rods yields 6.8 mol% Ca-Eskola component, which is consistent with the composition of the clinopyroxene inclusions in zircon. We conclude that the Ca-Eskola component in the peak metamorphic clinopyroxenes broke down by a retrograde reaction:

$$2\ Ca_{0.5}\square_{0.5}AlSi_2O_6 \rightarrow CaAl_2SiO_6 + 3\ SiO_2$$
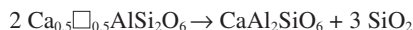
resulting in exsolution of the quartz rods in the matrix clinopyroxene.

Subducted crustal and supracrustal rocks form the Ca-Eskola clinopyroxene at high pressures and temperatures. The vacancy-containing clinopyroxene may have an important bearing on the physico-chemical properties of the subducted slab at upper mantle depth.

INTRODUCTION

Quartz rods have been observed in clinopyroxene of both eclogite and garnet clinopyroxenite of several ultrahigh-pressure (UHP) metamorphic belts (Smith 1984; Shatsky et al. 1985; Bakun-Czubarow 1992; Gayk et al. 1995; Zhang et al. 1995; Nakajima and Ogasawara 1998; Liou et al. 1998; Tsai and Liou 2000). Smith (1984) interpreted the quartz rods to be exsolution products from a pre-existing supersilicic clinopyroxene that contained excess silica at peak metamorphic conditions. Several experiments have demonstrated that the existence of supersilicic clinopyroxene requires high pressures and temperatures (e.g., Mao 1971; Khanukhova and Zharikov 1976; Wood and Henderson 1978; Zharikov et al. 1984; Gasparik 1986). Gayk et al. (1995) recalculated the composition of

clinopyroxene containing 2.6 wt% exsolved quartz from the Munchberg Massif, and derived a Ca-Na pyroxene with 10 mol% of the Ca-Eskola component ($Ca_{0.5}\square_{0.5}AlSi_2O_6$). This end-member was first hypothesized by Vogel (1966), based on the need to explain isochemical symplectic breakdown of omphacites to diopside plus feldspar. Smyth (1980) reported the presence of 17 mol% of the Ca-Eskola component in clinopyroxenes from eclogitic xenoliths in South African kimberlites. Sobolev et al. (1968) found marked deficiencies in cation sums of highly aluminous clinopyroxenes in kyanite eclogites from Siberian kimberlites.

Abundant quartz rods occur in clinopyroxene from eclogites from the Kumdykol region of the Kokchetav massif, Kazakhstan. The eclogite is intercalated with diamond-bearing gneiss. Zircon can protect peak metamorphic minerals from the effects of retrograde metamorphism, and is considered an excellent microcontainer for relict UHP phases because it is extremely stable and resistant over a wide temperature and pressure interval (e.g., Chopin and Sobolev 1995; Tabata et al.

1998). Therefore, we studied clinopyroxene inclusions in zircon separated from these rocks to ascertain the composition of the former clinopyroxene prior to silica exsolution. Approximately 400 zircon grains of about 70–80 μm in diameter from an eclogite (sample no. A21) and approximately 500 zircons of about 100 μm diameter from a biotite gneiss (sample no. A8) were separated and mounted in epoxy. Discrete inclusions in zircons were analyzed at the Tokyo Institute of Technology with a laser Raman spectrometer (JASCO NRS-2000) using the 514.5 nm line of an Ar-ion laser, and with a electron microprobe (JEOL JXA 8800) operated at 15 kV accelerating voltage, with a beam current of 12 nA and a beam diameter of 1 μm.

GEOLOGIC OUTLINE

The Kokchetav massif is situated in the central domain of the composite Eurasian craton (Fig. 1c), the major part of which was amalgamated and stabilized by a series of Paleozoic-Mesozoic collisional orogenic events (Dobretsov et al. 1995). It is composed of several Precambrian rock series, Cambro-Ordovician volcanic and sedimentary rocks, Devonian volcanic molasse, and Carboniferous-Triassic shallow-water and lacustrine sediments; these rocks were intruded by multi-stage granitic rocks (Dobretsov et al. 1995). This metamorphic belt is subdivided into four UHP-HP units and two low-pressure units; the UHP-HP units are structurally overlain by a low-grade metamorphic unit, and are underlain by the low-pressure facies series Daulet Suite (Kaneko et al. 1998). Metamorphic

diamonds have been identified in the Kumdykol region (Sobolev and Shatsky 1990; Katayama et al. 1998), which is situated in the central part of the Kokchetav massif (Fig. 1b). Intercalated biotite-gneiss, orthogneiss, eclogite, amphibolite and minor marble, quartzite, and Ti-clinohumite-bearing garnet peridotite crop out in this region (Shatsky et al. 1995; Kaneko et al. 1998: Fig. 1a). The eclogites occur as lenticular masses surrounding diamond-bearing rocks, and have yielded *P-T* conditions of > 6 GPa and > 1000 °C, applying the K_2O-in-augite geobarometer and Grt-Cpx geothermometer (Okamoto et al. 1998). Microdiamonds have been identified as inclusions in zircon, ganet, clinopyroxene, and kyanite in garnet-biotite gneiss, garnet-kyanite-phengite-quartz schist, and dolomitic marble (Sobolev and Shatsky 1990; Katayama et al. 1998). Other mineralogic indicators of UHP conditions of peak metamorphism, such as coesite, K-rich pyroxene, Si-rich phengite, and aluminous titanite are also present in rocks of the Kumdykol region (Shatsky et al. 1995; Zhang et al. 1997; Okamoto et al. 1998).

MINERAL PARAGENESIS

The eclogite (A21) consists of garnet (70 modal%) + omphacite (20 modal%) + rutile (< 2 modal%) + quartz (5 modal%), with minor amounts of apatite and zircon (Fig. 2a). Amphibole, ilmenite, albite, and potassium feldspar are present as retrograde phases. Most omphacite grains contain crystallographically oriented quartz rods, which are a few micrometers in diameter and about 100 μm in length (Fig. 2b). Some
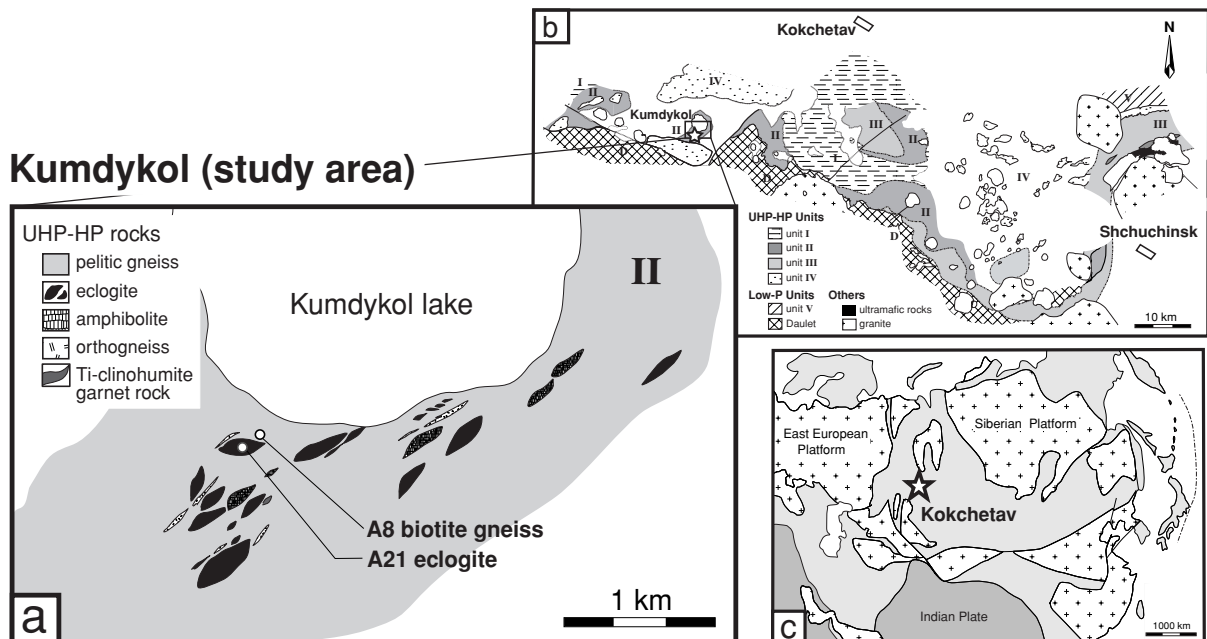

FIGURE 1. (a) The distribution of lithologies with sample localities in the Kumdykol region. **(b)** Simplified geological map of the Kokchetav Massif, modified after Kaneko et al. (1998). **(c)** Simplified map of Eurasian craton showing the locality of the Kokchetav Massif.

TABLE 1. Mineral paragenesis in matrix and zircon

Sample	Dia	Coe	Gr	Qtz	Cpx	Grt	Rt	Ky	Phn	Amp	Ilm	Kfs	Ab	Bt	Chl	Ap	Zr
A21 eclogite																	
Matrix				+	+	+	+			s	s	s	s			+	+
Inclusion in zircon		+		+	+	+	+						+				
A8 biotite gneiss																	
Matrix			+	+		+	+		s		+			+	s	+	+
Inclusion in zircon	+	+	+	+	+	+	+	+	+				+			+	

Notes: s = secondary mineral; Dia = diamond, Coe = coesite, Gr = graphite, Qtz = quartz, Cpx = clinopyroxene, Grt = garnet, Rt = rutile, Ky = kyanite, Phn = phengite, Amp = amphibole, Ilm = ilmenite, Kfs = Potassium feldspar, Ab = albite, Bt = biotite, Chl = chlorite, Ap = apatite, Zr = zircon.
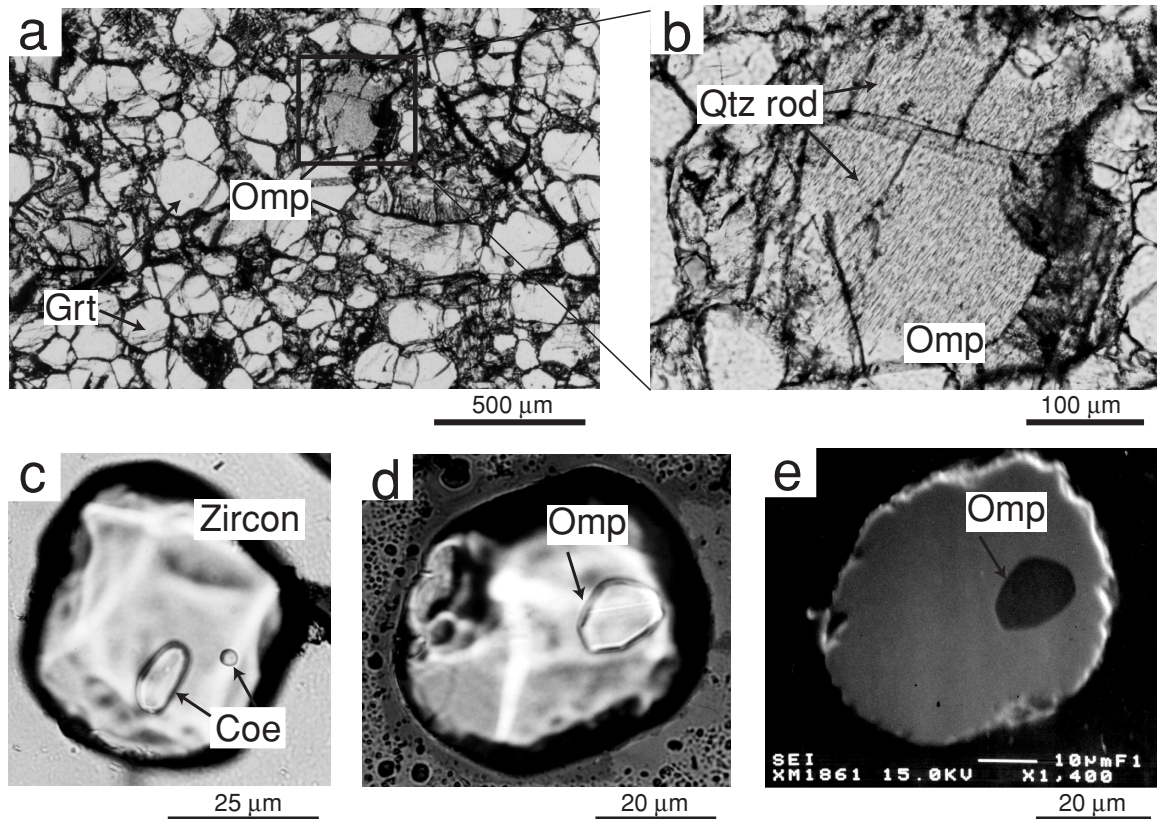

FIGURE 2. Photomicrographs showing mineral assemblages and inclusions in zircon (in plane-polarized light). (**a**) Mineral assemblage in A21 eclogite consists mainly of garnet (Grt) and omphacite (Omp). (**b**) Expanded photomicrograph shows quartz (Qtz) rods in omphacite. The rods display a consistent crystallographic orientation. (**c**) Coesite (Coe) inclusion in zircon from A21 eclogite. (**d**) Omphacite inclusion in zircon in the eclogite. (**e**) Secondary electron image of the omphacite inclusion and host zircon.

omphacite grains are replaced at the rims by symplectitic intergrowths of augite and plagioclase. Garnets are mostly homogeneous ($Alm_{42}Grs_{36}Prp_{21}Sps_1$), and contain significant amounts of Na (up to 0.15 wt% Na_2O) and Ti (up to 0.4 wt% TiO_2). The significance of Na in garnet coexisting with Na-bearing minerals has been discussed by Sobolev and Lavrentiev (1971) and considered by them to be indicative of very high pressure. However, coesite was not detected in the matrix of the eclogite. Inclusions in zircon comprise omphacite, garnet, coesite, rutile, quartz, and albite, in decreasing order of abun-

dance, which are approximately 5–20 μm in size (Table 1). Both high-pressure and low-pressure mineral inclusions occur together in a single rock sample. Katayama et al. (1998) concluded that inclusions in zircon are representative of both the prograde and peak metamorphic assemblages. Coesite inclusions are ovoid, and approximately 10 μm in diameter (Fig. 2c); they yield the characteristic Raman band at 523 cm^{-1} and weaker bands at 271, 181, and 149 cm^{-1}. Quartz rods are absent in omphacite inclusions that are approximately 10 μm in diameter (Figs. 2d and 2e). Garnet inclusions have slightly

TABLE 2. Representative compositions of clinopyroxene

Rock sample	A21 eclogite Inclusion in zircon				Matrix				A8 biotite gneiss Inclusion in zircon	
Sample no.	E3-1	E71-1	E132-2	E134-2	EG2	EG32	EG33	EG36	B69-1	B2-1
wt% oxides										
SiO_2	55.55	55.75	55.82	55.62	55.55	55.64	55.67	55.76	58.58	57.48
TiO_2	0.26	0.24	0.18	0.08	0.17	0.13	0.15	0.17	0.23	0.14
Al_2O_3	9.68	9.70	10.17	9.63	9.63	9.78	9.91	9.52	18.84	19.32
Cr_2O_3	0.00	0.00	0.00	0.00	0.02	0.05	0.00	0.00	0.04	0.00
FeO	5.44	5.89	5.56	5.44	5.70	5.66	5.65	5.81	2.37	2.37
MnO	0.01	0.05	0.00	0.04	0.05	0.02	0.00	0.04	0.09	0.12
MgO	8.59	8.56	8.90	8.93	8.89	8.90	8.85	9.10	4.35	3.85
CaO	14.97	14.45	14.25	14.49	14.18	14.33	13.76	14.37	7.53	6.39
Na_2O	4.84	5.32	5.26	5.32	5.58	5.60	5.88	5.33	8.79	9.57
K_2O	0.04	0.07	0.00	0.05	0.12	0.09	0.02	0.04	0.00	0.00
Total	99.38	100.02	100.14	99.58	99.90	100.20	99.89	100.12	100.83	99.24
Cations per six oxygen atoms										
Si	1.999	1.998	1.992	1.999	1.994	1.991	1.995	1.996	1.997	1.990
Ti	0.007	0.006	0.005	0.002	0.005	0.003	0.004	0.005	0.006	0.004
Al	0.410	0.410	0.427	0.408	0.408	0.413	0.418	0.401	0.757	0.789
Cr	0.000	0.000	0.000	0.000	0.001	0.002	0.000	0.000	0.001	0.000
Fe^{2+}	0.164	0.177	0.166	0.163	0.171	0.169	0.169	0.174	0.068	0.069
Mn	0.000	0.001	0.000	0.001	0.001	0.001	0.000	0.001	0.003	0.004
Mg	0.461	0.458	0.473	0.478	0.476	0.475	0.473	0.485	0.221	0.199
Ca	0.577	0.555	0.545	0.558	0.545	0.549	0.528	0.551	0.275	0.237
Na	0.338	0.370	0.364	0.371	0.389	0.388	0.408	0.370	0.581	0.643
K	0.002	0.003	0.000	0.002	0.006	0.004	0.001	0.002	0.000	0.000
Total	3.959	3.977	3.972	3.982	3.995	3.995	3.997	3.985	3.909	3.933

higher Grs contents than garnets in the matrix, and contain significant Na (up to 0.09 wt% Na_2O) and Ti (up to 0.35 wt% TiO_2).

The biotite gneiss (A8) consists of garnet (20 modal%) + biotite (20 modal%) + phengite (< 5 modal%) + quartz (50 modal%), with minor rutile, ilmenite, zircon, and apatite. Garnet is commonly fractured, and replaced by biotite and chlorite. Garnet shows reverse zoning with Prp contents decreasing from core (24–26 mol%) to rim (19–25 mol%), and contains significant amounts of Na (up to 0.19 wt% Na_2O). Inclusions in zircons include microdiamond, coesite, garnet, jadeitic pyroxene, phengite, kyanite, apatite, albite, graphite, and quartz, which are approximately 5–30 µm in size (Table 1). Microdiamonds are usually about 10 µm in diameter, the largest being 24 µm, and yield the characteristic Raman band at 1333 cm^{-1}. The clinopyroxene inclusions are rare and relatively small, at 5 µm in diameter.

CLINOPYROXENE COMPOSITIONS

Zircon-hosted clinopyroxene from both the eclogite and biotite-gneiss exhibit an excess of Fe^{3+} + ^{VI}Al over ^{IV}Al + Na + K, and calculated cation totals of significantly less than 4.0 per six O atoms. All analyzed grains show substantial excess ^{VI}Al. For microprobe analyses, total Fe is reported as Fe^{2+}; if Fe^{3+} is present, the cation deficiency would be even greater (Kushiro and Aoki 1968). We calculated Fe^{3+} contents based on four cations and the charge-balance constraint of Droop (1987). An alternative approach that assumes Fe^{3+} = Na – (Al – 2^{IV}Al – K) yielded slightly higher Fe^{3+} contents, but generally not by more than 10%. However, it is impossible to calculate the Fe^{3+} con-

tents from stoichiometric considerations if substantial numbers of vacancies exist in the structure (e.g., Mysen and Griffin 1973; Cawthorn and Collerson 1974; Droop 1987). Table 2 presents compositions of four clinopyroxenes in zircon and four in the matrix from the eclogite, and two clinopyroxenes in zircon from the diamond-bearing biotite-gneiss. Most analyses of clinopyroxene inclusions in zircon indicate nearly sufficient silica to occupy the tetrahedral site, so that there is relatively little ^{IV}Al; the excess Al cannot be ascribed to the Ca-Tschermak component. The calculated cations indicate that a deficiency is maintained only by a significant portion of M-site vacancies. The stoichiometry of these pyroxenes can be reconciled best by consideration of the end-member Ca-Eskola component ($Ca_{0.5}\square_{0.5}AlSi_2O_6$, where $\square$ is a vacancy on the M_2 site). We assumed eight pyroxene end-members: Ca-Eskola (CaEs), Ca-Tschermak (CaTs), jadeite (Jd), acmite (Acm), augite (Aug, diopside + hedenbergite), orthopyroxene (Opx, enstatite + ferrosilite), $Na(Mg,Fe)_{0.5}Ti_{0.5}Si_2O_6$ and $KAlSi_2O_6$. The end-member calculations were based on the method of Smyth (1980), with several modifications. The Fe^{3+} content (Acm) was calculated on the basis of charge balance constraint for six O atoms. The Ca-Tschermak component was assigned to be equivalent to ^{IV}Al content, which is determined by 2-Si, because only Al and Si are permitted in the T sites. All Ti was assumed to occupy the M_1 site in $Na(Mg,Fe)_{0.5}Ti_{0.5}Si_2O_6$. Therefore, the jadeite component was calculated from the method: Na-Fe^{3+}-2Ti. K was assumed to occupy the M_2 site in $KAlSi_2O_6$. Any remaining ^{VI}Al was assigned to the Ca-Eskola component, which was calculated from the method: Al-2^{IV}Al-K-(Na-Fe^{3+}-2Ti). The augite and orthopyroxene components were calcu-

FIGURE 3. Cation total (on the basis of six O atoms) vs. Ca-Eskola component of clinopyroxenes in zircon from eclogite (A21) and biotite gneiss (A8), and in matrix of eclogite (A21). Clinopyroxenes in eclogitic xenoliths in South Africa kimberlites reported by Smyth (1980) are also plotted for comparison. Reference line is the ideal relation between the Ca-Eskola component and vacancy.
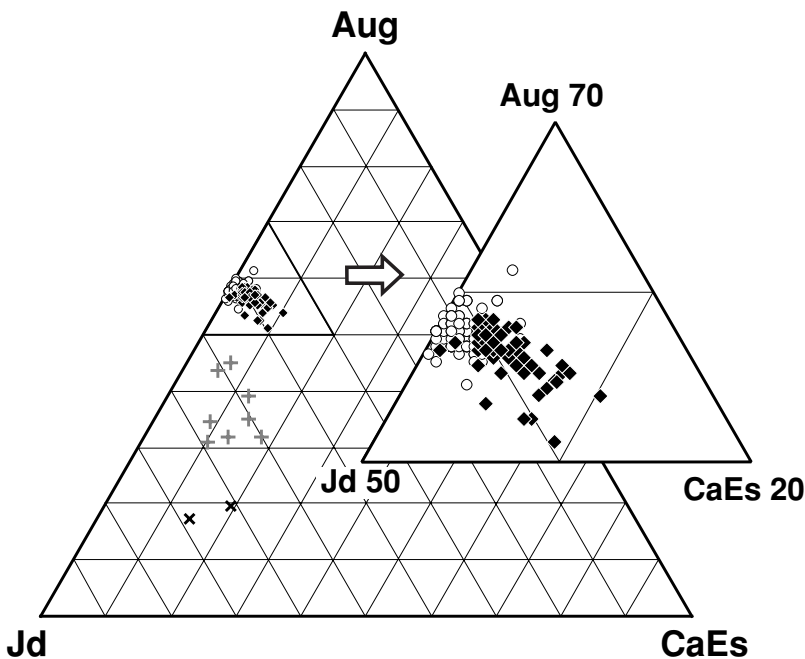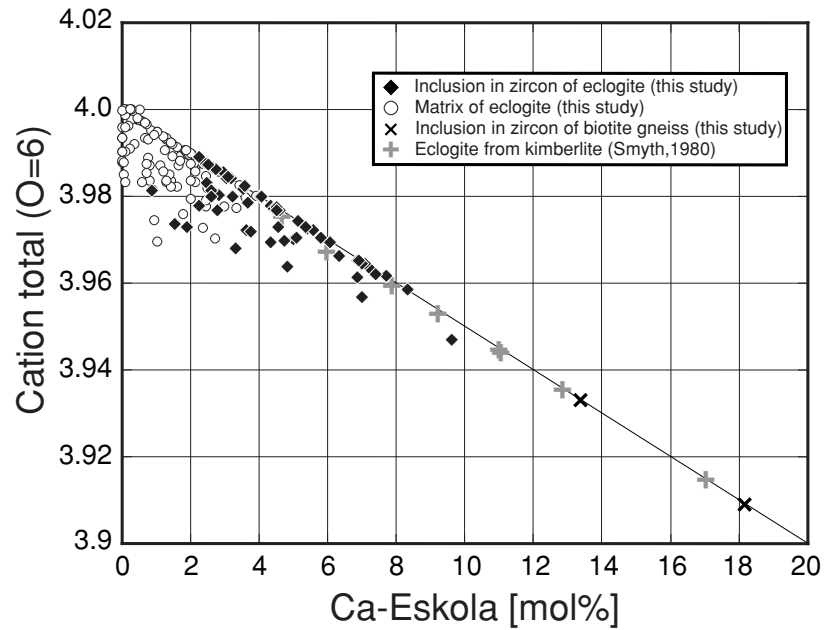

FIGURE 4. Clinopyroxene compositions plotted on a Augite (Aug)–Jadeite (Jd)–Ca-Eskola (CaEs) ternary diagram. The symbols are the same as in Figure 3.

lated as Ca-2CaTs-0.5CaEs and (Mg + Fe²⁺ – Ti – Aug)/2, respectively.

Figure 3 shows cation totals (O = 6) vs. Ca-Eskola component of the Kokchetav clinopyroxenes compared with clinopyroxenes from South African kimberlite reported by Smyth (1980). The clinopyroxene inclusion in zircon contains significant amounts of the Ca-Eskola component; up to 9.6 mol% with an average of 4.6 mol% for 58 grains in eclogite,

and 18.2 mol% in diamond-bearing biotite gneiss. On the other hand, the matrix clinopyroxene contains substantially less (average of 1.3 mol% from 97 analyses). The amount of the Ca-Eskola component increases with the number of vacancies (4 cation total), whereas it is calculated independent of vacancies from the relationship, Al-2^{IV}Al-K-(Na-Fe^{3+}-2Ti). This finding indicates that the Ca-Eskola component can account for the clinopyroxene compositions.

The reference line for the Ca-Eskola component and vacancies is also shown in Figure 3. Some analyses plots below this reference line, which may result from either analytical error or another vacancy in the M_1 site as postulated by Wood and Henderson (1978).

We recalculated the compositions of matrix clinopyroxenes in eclogite that have an estimated 2.1 wt% quartz rods based on analyses of backscattered electron images, 2000 μm^2 in area. The recalculated precursor pyroxene contains 6.8 mol% of the Ca-Eskola component, which is consistent with the composition of the clinopyroxene inclusions in zircon. Figure 4 shows the clinopyroxene compositions plotted on a ternary Augite–Jadeite–Ca-Eskola diagram. The clinopyroxene from the eclogite plots in the omphacite field, and that from the biotite gneiss in the jadeite field. The zircon-hosted omphacite of the eclogite displays a trend extending to the Ca-Eskola end-member, whereas the matrix clinopyroxene is almost homogeneous. The clinopyroxene in eclogite generally contains 4–6 mol% of the Opx component; zircon-hosted clinopyroxene is slightly higher (up to 8.8 mol%). The amount of the Ca-Tschermak component is minor, but relatively higher in the matrix (up to 2.6 mol%).

K_2O solubility in clinopyroxene is an important indicator of UHP conditions (e.g., Schmidt 1996; Luth 1997; Okamoto and Maruyama 1998); high-K_2O clinopyroxene has been reported for diamond-grade eclogite of the Kumdykol region (Shatsky et al. 1995; Zhang et al. 1997; Okamoto et al. 1998). The analyzed clinopyroxene in our eclogite sample also contains significant amounts of K_2O—up to 0.21 wt% in zircon and 0.16 wt% in the matrix.

DISCUSSION

As described above, exsolved quartz is restricted to matrix clinopyroxenes that show significant compositional differences compared with clinopyroxene inclusions in zircon. These features suggest that quartz exsolution is related to breakdown of the Ca-Eskola component. The clinopyroxene in zircon contains relatively higher amounts of the Ca-Eskola component than that in the matrix, which is consistent with recalculation of the precursor composition of the matrix clinopyroxene containing quartz rods. The vacancy-containing Ca-Eskola clinopyroxene is reported to be pressure sensitive and highly unstable at lower pressure (Mao 1971; Smyth 1980). We conclude that the Ca-Eskola component, which existed at peak metamorphic conditions, broke down by the retrograde reaction:

$$2\ Ca_{0.5}\square_{0.5}AlSi_2O_6 \rightarrow CaAl_2SiO_6 + 3\ SiO_2$$
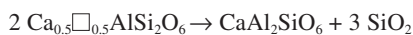
This reaction resulted in exsolution of quartz rods in the matrix clinopyroxene, and an increase of the Ca-Tschermak component. However, the precise $P\text{-}T$ condition of the reaction is still debated (Mao 1971; Khanukhova and Zharikov 1976; Wood and Henderson 1978; Zharikov et al. 1984; Gasparik 1986). Further experiments concerning the Ca-Eskola clinopyroxene will constrain the retrograde $P\text{-}T$ conditions, and the solubility of this component in clinopyroxene could potentially be a new geobarometer for UHP metamorphic rocks, similar to solubilities of K in clinopyroxene and Na in garnet.

Transportation of water from the subducted slab into the mantle has been of considerable interest to many earth scientists (e.g., Bell and Rossman 1992; Schmidt and Poli 1998; Okamoto and Maruyama 1999), because water plays an important role in determining the properties of minerals and melt generation in the Earth's upper mantle. The main hydrous minerals in the subducted slab, phlogopite, zoisite, and amphibole, are not believed to exist in significant quantities at depth. Some of the less-abundant phases found in subducted rocks contain small amounts of hydrous components (Rossman and Smyth 1990; Bell and Rossman 1992), but do not constitute important reservoirs for water. However, Smyth et al. (1991) reported that pyroxene containing the Ca-Eskola component from the Roberts Victor kimberlite xenolith contains up to 1000 ppm OH. This hydroxyl has been reported to be associated with cation vacancies in clinopyroxene (Smyth et al. 1991). This finding suggests that the Ca-Eskola pyroxene may be an important reservoir for hydrous components in the upper mantle. By extrapolating the experimental data curve of Smyth et al. (1991), we interpret the Kokchetav clinopyroxenes in eclogite to contain as much as 1500 ppm hydroxyl and those in pelitic gneiss up to 2500 ppm. According to mineral proportions, the bulk eclogite may contain approximately 800 ppm hydroxyl, even though no hydrous minerals exist in the rock. Thus, clinopyroxene in deeply subducted crustal rocks can carry a significant amount of water into the mantle, and have an important bearing on the physico-chemical properties of the slab at great depth.

REFERENCES CITED

Bakun-Czubarow, N. (1992) Quartz pseudomorphs after coesite and quartz exsolutions in eclogitic omphacites of the Zlote Mountains in the Sudetes (SW Poland). Archiwum Mineral, 49, 3–25.

Bell, D.R. and Rossman, G.R. (1992) Water in Earth's Mantle: The role of nominally anhydrous minerals. Science, 255, 1391–1397.

Cawthorn, R.G. and Collerson, K.D. (1974) The recalculation of pyroxene end-member parameters and the estimation of ferrous and ferric iron content from electron microprobe analyses. American Mineralogist, 59, 1203–1208.

Chopin, C. and Sobolev, N.V. (1995) Principal mineralogic indicator of UHP in crustal rocks. In Coleman, R.G. and Wang, X. eds. Ultrahigh-Pressure Metamorphism, 96–133. Cambridge University Press, Cambridge.

Dobretsov, N.L., Sobolev, N.V. Shatsky, V.S., Coleman, R.G., and Ernst, W.G. (1995) Geotectonic evolution diamondiferous paragneisses, Kokchetav Complex, Northern Kazakhstan: The geologic enigma of ultrahigh-pressure crustal rocks within a Paleozoic foldbelt. Island Arc, 4, 267–279.

Droop, G.T.R. (1987) A general equation for estimating Fe^{3+} concentrations in ferromagnesian silicates and oxides from microprobe analyses, using stoichiometric criteria. Mineralogical Magazine, 51, 431–435.

Gasparik, T. (1986) Experimental study of subsolidus phase relations and mixing properties of clinopyroxene in the silica-saturated system $CaO\text{-}MgO\text{-}Al_2O_3\text{-}SiO_2$. American Mineralogist, 71, 686–693.

Gayk, T., Kleinschrodt, R., Langosch, A., and Seidel, E. (1995) Quartz exsolution in clinopyroxene of high-pressure granulite from the Munchberg Massif. European Journal of Mineralogy, 7, 1217–1220.

Kaneko, Y., Maruyama, S., Terabayashi, M., Yamamoto, H., Ishikawa, M., Anma,

R., Parkinson, C.D., Ohta, T. Nakajima, Y. Katayama, I., Yamamoto, J., Masago, H., Liou, J.G., and Ogasawara, Y. (1998) Geology of the Kokchetav UHP-HP units, northern Kazakhstan. EOS Transactions, AGU fall meeting, 79, F983.

Katayama, I., Zayachkovsky, A.A., and Maruyama, S. (1998) Mineral inclusions in zircon from Kokchetav Massif, northern Kazakhstan. EOS Transactions, AGU fall meeting, 79, F988.

Khanukhova, L.T. and Zharikov, V.A. (1976) Excess silica in solid solutions of high-pressure clinopyroxenes as shown by experimental study of the system $CaMgSi_2O_6$-$CaAl_2SiO_6$ at 35 kilobars and 1200 °C. Doklady Academy of Sciences USSR, Earth Science Section, 229, 170–172.

Kushiro, I. and Aoki, K. (1968) Origin of some eclogite inclusions. American Mineralogist, 53, 1347–1367.

Liou, J.G., Zhang, R.Y., Ernst, W.G., Rumble, D., and Maruyama, S. (1998) High-pressure minerals from deeply subducted metamorphic rocks. Ultrahigh-pressure mineralogy: physics and chemistry of the Earth's deep interior. Reviews in Mineralogy, 37, 33–96.

Luth, R.W. (1997) Experimental study of the system phlogopite-diopside from 3.5 to 17 GPa. American Mineralogist, 82, 1198–1209.

Mao, H.K. (1971) The system jadeite ($NaAlSi_2O_6$)–anorthite ($CaAl_2Si_2O_8$) at high pressures. Carnegie Institute Year Book, 69, 163–168.

Mysen, B. and Griffin, W.L. (1973) Pyroxene stoichiometry and the breakdown of omphacite. American Mineralogist, 58, 60–63.

Nakajima, Y. and Ogasawara, Y. (1998) Petrology of eclogite and Ti-clinohumite bearing rock from Kumdykol, Kokchetav Massif, Kazakhstan—some mineralogical records of UHP conditions. Abstract of Japan Geological spring meeting, 106, 52.

Okamoto, K. and Maruyama, S. (1998) Multi-anvil re-equilibration experiments of a Dabie Shan ultrahigh-pressure eclogites within the diamond-stability fields. Island Arc, 7, 52–69.

———(1999) The high-pressure synthesis of lawsonite in the MORB + H_2O system. American Mineralogist, 84, 362–373.

Okamoto, K., Maruyama, S., Liou, J.G., and Ogasawara, Y. (1998) Petrological study of the diamond-grade eclogite in the Kokchetav massif, northern Kazakhstan. EOS Transactions, AGU fall meeting, 79, F988.

Rossman, G.R. and Smyth, J.R. (1990) Hydroxyl contents of accessory minerals in mantle eclogites and related rocks. American Mineralogist, 75, 775–780.

Schmidt, M.W. (1996) Experimental constraints on recycling of potassium from subducted oceanic crust. Science, 272, 1927–1930.

Schmidt, M.W. and Poli, S. (1998) Experimentally based water budgets for dehydrating slabs and consequences for arc magma generation. Earth and Planetary Science Letters, 163, 361–379.

Smith, D.C. (1984) Coesite in clinopyroxene in the Caledonides and its implications for geodynamics. Nature, 310, 641–644.

Smyth, J.R. (1980) Cation vacancies and the crystal chemistry of breakdown reactions in kimberlitic omphacites. American Mineralogist, 65, 1185–1191.

Smyth, J.R., Bell, D.R., and Rossman, G.R. (1991) Incorporation of hydroxyl in upper-mantle clinopyroxenes. Nature, 351, 732–735.

Shatsky, V.S., Sobolev, N.V., and Stenina, N.G. (1985) Structural peculiarities of pyroxenes from eclogites. Terra Cognita, 5, 436–437.

Shatsky, V.S., Sobolev, N.V., and Vavilov, M.A. (1995) Diamond-bearing metamorphic rocks of the Kokchetav massif (northern Kazakhstan). In Coleman, R.G. and Wang, X. eds. Ultrahigh-Pressure Metamorphism, 427–455. Cambridge University Press, Cambridge.

Sobolev, N.V. and Lavrentiev, Y.G. (1971) Isomorphic sodium admixture in garnets formed at high pressure. Contributions to Mineralogy and Petrology, 31, 1–12.

Sobolev, N.V. and Shatsky, V.S. (1990) Diamond inclusion in garnets from metamorphic rocks. Nature, 343, 742–746.

Sobolev, N.V., Kuznetsova, I.K., and Zyuzin, N.I. (1968) The petrology of grospydite xenoliths from Zagodochnaya kimberlite pipe in Yakutia. Journal of Petrology, 9, 253–280.

Tabata, H., Yamauchi, K., Maruyama, S., and Liou, J.G. (1998) Tracing the extent of a UHP metamorphic terrane: mineral-inclusion study of zircons in gneiss from the Dabie Shan. In B.R. Hacker and J.G. Liou, Eds., When Continents Collide: Geodynamics and Geochemistry of Ultrahigh-Pressure Rocks, 261–273. Kluwer Academic Publishers, London.

Tsai, C.H. and Liou, J.G. (2000) Eclogite-facies relics and inferred ultrahigh-pressure metamorphism in the North Dabie Complex, central-eastern China. American Mineralogist, 85, 1–8.

Vogel, D.E. (1966) Nature and chemistry of the formation of clinopyroxene-plagioclase symplectite from omphacite. Neues Jahrbuch für Mineralogie Monatshefte, 185–189.

Wood, B.J. and Henderson, C.M.B. (1978) Compositions and unit-cell parameters of synthetic non-stoichiometric tschermakitic clinopyroxenes. American Mineralogist, 63, 66–72.

Zhang, R.Y., Hirajima, T., Banno, S., Cong, B. and Liou, J.G. (1995) Petrology of ultrahigh-pressure rocks from the southern Sulu region, eastern China. Journal of Metamorphic Geology, 13, 659–675.

Zhang, R.Y., Liou, J.G., Ernst, W.G., Coleman, R.G., Sobolev, N.V. and Shatsky, V.S. (1997) Metamorphic evolution of diamond-bearing and associated rocks from the Kokchetav massif, northern Kazakhstan. Journal of Metamorphic Geology, 15, 479–496.

Zharikov, V.A., Ishbulatov, R.A. and Chudinovskikh, L.T. (1984) High-pressure clinopyroxenes and the eclogite barrier. Soviet Geology and Geophysics, 25, 53–61.